Tohoku J. Exp. Med., 2019, **249**, 19-28

# Flow Cytometry-Based Photodynamic Diagnosis with 5-Aminolevulinic Acid for the Detection of Minimal Residual Disease in Multiple Myeloma

**Keita Iwaki,[1] Tohru Fujiwara,[2,3] Takako Ito,[1] Chie Suzuki,[2] Katsuyuki Sasaki,[2] Koya Ono,[3] Kei Saito,[3] Noriko Fukuhara,[3] Yasushi Onishi,[3] Hisayuki Yokoyama,[3] Shinichi Fujimaki,[2] Tohru Tanaka,[4] Hideto Tamura,[5] Minami Fujiwara[1] and Hideo Harigae[1,2,3]**

[1]Division of Blood Transfusion and Cell Processing, Tohoku University Hospital, Sendai, Miyagi, Japan
[2]Laboratory Diagnostics, Tohoku University Hospital, Sendai, Miyagi, Japan
[3]Department of Hematology and Rheumatology, Tohoku University Graduate School of Medicine, Sendai, Miyagi, Japan
[4]SBI Pharmaceuticals Co., Ltd., Tokyo, Japan
[5]Department of Hematology, Nippon Medical School, Tokyo, Japan

Multiple myeloma is the cancer of plasma cells. Along with the development of new and effective therapies, improved outcomes in patients with multiple myeloma have increased the interest in minimal residual disease (MRD) monitoring. However, the considerable heterogeneity of immunophenotypic and molecular markers of myeloma cells has limited its clinical application. 5-Aminolevulinic acid (ALA) is a natural compound in the heme biosynthesis pathway. Following ALA treatment, tumor cells preferentially accumulate porphyrins because of the differential activities of aerobic glycolysis, known as Warburg effect. Among various porphyrins, protoporphyrine IX is a strong photosensitizer; thus, ALA-based photodynamic diagnosis has been widely used in various solid cancers. Here, the feasibility of flow cytometry-based photodynamic detection of MRD was tested in multiple myeloma. Among various human cell lines of hematological malignancies, including K562 erythroleukemia, Jurkat T-cell leukemia, Nalm6 pre-B cell leukemia, KG1a myeloid leukemia, and U937 monocytic leukemia, human myeloma cell line, KMS18, and OPM2 abundantly expressed ALA transporters, such as *SLC36A1* and *SLC15A2*, and 1 mM ALA treatment for 24 h resulted in nearly 100% porphyrin fluorescence expression, which could be competitively inhibited by ALA transport with gamma-aminobutyric acid. Titration studies revealed that the lowest ALA concentration required to achieve nearly 100% porphyrin fluorescence in KMS18 cells was 0.25 mM, with an incubation period of 2 h. Under these conditions, incubation of primary peripheral blood mononuclear cells resulted in only 1.8 % of the cells exhibiting porphyrin fluorescence. Therefore, flow cytometry-based photodynamic diagnosis is a promising approach for detecting MRD in multiple myeloma.

**Keywords:** 5-aminolevulinic acid; flow cytometry; minimal residual disease; multiple myeloma; protoporphyrin IX
Tohoku J. Exp. Med., 2019 September, **249** (1), 19-28. 

## Introduction

5-aminolevulinic acid (ALA), an important precursor of heme, is a natural amino acid synthesized in the mitochondria of both animals and plants (Ishizuka et al. 2011). It is synthesized from glycine and succinyl-CoA in the mitochondria and catalyzed by two different ALA synthases (ALAS): one expressed ubiquitously (ALAS1) and the other expressed by erythroid precursors (ALAS2) only (Furuyama et al. 2007). ALA is exported to the cytosol during synthesis, where it is converted to coproporphyrinogen III. The remaining steps of heme biosynthesis occur inside the mitochondria. Coproporphyrinogen III is imported to the mitochondria and finally catalyzed into protoporphyrin IX (PpIX). Subsequently, heme is generated by inserting ferrous iron into protoporphyrin IX, which is then catalyzed by ferrochelatase (FECH). Exogeneous ALA administration bypasses ALAS regulation and saturates FECH, resulting in PpIX accumulation (Ishizuka et al. 2011). Tumor cells have been known to preferentially accumulate PpIX upon ALA administration, by increasing ALA uptake and perhaps decreasing FECH activity, known

Received July 16, 2019; revised and accepted August 28, 2019. Published online September 12, 2019; doi: 10.1620/tjem.249.19.
Correspondence: Tohru Fujiwara, M.D., Ph.D., Department of Hematology and Rheumatology, Tohoku University Graduate School of Medicine, 2-1 Seiryo-machi, Aoba-ku, Sendai, Miyagi 980-8575, Japan.
e-mail: fujiwara-to@med.tohoku.ac.jp

as the "Warburg effect" (Warburg 1956). Because PpIX is an active photosensitizer, ALA-based photodynamic diagnosis has been used for various cancers (Gibbs et al. 2006; Ishizuka et al. 2011; Nokes et al. 2013).

Multiple myeloma is a type of cancer of plasma cells, a type of white blood cells that normally produce antibodies (Paiva et al. 2015). With the development of new and effective therapies that significantly contribute to improved outcomes, the majority of patients with multiple myeloma will inevitably relapse (Paiva et al. 2015). Therefore, detection of minimal residual disease (MRD) has recently become essential to assess the treatment effectiveness against multiple myeloma (Paiva et al. 2015; Gambella et al. 2019). To date, several techniques have been explored, as represented by multicolor flow cytometry- and next-generation sequencing-based MRD detections (Paiva et al. 2015; Gambella et al. 2019). Both techniques exhibited high sensitivity in detecting myeloma cells ($10^{-5}$ to $10^{-6}$) (Paiva et al. 2015); however, their clinical application has currently been quite limited. The multicolor flow cytometry utilizes a complex combination of multiple antibodies, thereby requiring further technical standardization, whereas the next-generation sequencing could not be applied to all patients with myeloma owing to the availability of tumor-specific molecular markers as well as the accessibility of specialized facilities for comprehensive sequencing (Paiva et al. 2015; Anderson et al. 2017; Gambella et al. 2019). Thus, more simple and versatile techniques should be used.

ALA-based photodynamic diagnosis has been used for various solid cancers, such as breast and brain (Ishizuka et al. 2011; Nokes et al. 2013). In this application, ALA should be systemically administered orally and intravenously (Ishizuka et al. 2011; Nokes et al. 2013). However, PpIX fluorescence could possibly be detected using flow cytometry. In the latter situation, ALA could be used as an *ex vivo* treatment, thereby reducing the need for systemic ALA administration. Thus, this study explored the potential usefulness of flow cytometry-based detection of MRD in multiple myeloma.

## Material and Methods

*Cell culture and reagents*

OPM2 and KMS18, human multiple myeloma cell lines, were obtained from DSMZ-German Collection of Microorganisms and Cell Culture (Braunschweig, Germany) and Dr. Otsuki (Kawasaki Medical School, Okayama, Japan), respectively. K562 erythroleukemia cell line, human T-cell leukemia cell line Jurkat, human pre-B-cell leukemia cell line Nalm6, myeloid leukemia cell line KG1a, and human monocytic cell line U937 were acquired as previously described (Saito et al. 2015). ALA hydrochloride (SBI Pharmaceuticals Co., Ltd., Tokyo, Japan) and gamma-aminobutyric acid (GABA) (Sigma) were prepared with distilled water. All cells were cultured in the RPMI-1640 medium, containing 10% fetal bovine serum (Biowest, Miami, FL) and 1% penicillin-streptomycin (Sigma, St. Louis, MO, USA) in a humidified incubator at 37°C with 5% carbon dioxide.

*Preparation of human peripheral blood mononuclear cell (PBMC)*

To obtain PBMCs, fresh whole blood samples from a single normal volunteer were collected in an ethylenediamine tetraacetic acid (EDTA)-treated tube, and overlaid on Ficoll-Paque PLUS (GE Healthcare, Uppsala, Sweden) and subjected to centrifugation at 1,500 rpm for 30 min at room temperature. After removing the upper layer, the mononuclear cells were washed twice with phosphate-buffered saline (PBS), and were seeded in the RPMI-1640 medium, containing 10% fetal bovine serum (Biowest) and 1% penicillin-streptomycin (Sigma). The study was approved by ethical committee of Tohoku University Graduate School of Medicine.

*Real-time quantitative reverse transcription-polymerase chain reaction (RT-PCR)*

The total RNA was purified using TRIzol (Invitrogen), and 1 $\mu$g of purified total RNA was used to synthesize the complementary DNA (cDNA) using the ReverTra Ace qPCR-RT Master Mix (TOYOBO). Reaction mixtures (20 $\mu$L) for real-time quantitative RT-PCR comprised 2 $\mu$L of cDNA, 10 $\mu$L of Quantitect SYBR Green PCR Master Mix (QIAGEN), and appropriate primers. Reaction program is as follows; 94°C (denature) for 30 sec, 60°C (annealing) for 30 sec, and 72°C (extension) for 30 sec using C1000 Thermal Cycler CFX96™ Real-Time system (Bio-Rad laboratories, Hercules, CA, USA). Product accumulation was monitored by measuring the SYBR Green fluorescence and was normalized according to *GAPDH* messenger RNA (mRNA).

To evaluate the expression levels of human ALA transporters [i.e., solute carrier family 36 (proton/amino acid symporter), member (SLC36A1); solute carrier family 15 (oligopeptide transporter), members (SLC15A1 and SLC15A2); and *solute carrier* family 6 (neurotransmitter transporter), *member 13* (SLC6A1)], an amplified cDNA fragment of each gene was cloned using the pGEM™-T Easy Vector (Promega, Madison, WI), which was used as an internal standard in quantitative RT-PCR. The plasmid copy number was calculated as follows: copy number (copy/$\mu$L) = $6.02 \times 10^{23} \times$ [plasmid DNA concentration ($\mu$g/$\mu$L)] $\times 10^{-6}$/ [total plasmid size (base pair)] $\times$ 660. Primer sequences are shown in Table 1.

*Flow cytometry*

The RPMI-1640 medium containing ALA was used to incubate cells, which were subsequently washed with phosphate-buffered saline. Protoporphyrin IX (PpIX) fluorescence was measured using BD FACSAria II flow cytometers (BD Biosciences, Franklin Lakes, NJ, USA) with an excitation and emission wavelengths of 488 nm and 685-735 nm, respectively. Phycoerythrin-conjugated antibodies against human CD3 (clone SP34-2), CD14 (clone M5E2), and CD19 (clone HIB19) were purchased from BD pharmingen (BD Biosciences).

## Results and Discussion

*Multiple myeloma cell lines preferentially accumulate ALA-induced PpIX*

First, a quantitative RT-PCR analysis of previously identified ALA transporters was performed based on various cell lines of hematological malignancy. Two proton-coupled oligopeptide transporters (SLC15A1, peptide transporter [PepT] 1, and SLC15A2, PepT2) (Ahlin et al. 2009, Ingersoll et al. 2012), a human proton-coupled amid acid

Table 1. Oligonucleotide primers for RT-PCR.

| Gene | Direction | Sequence (5′ → 3′) | Amplicon length(bp) |
|---|---|---|---|
| *GAPDH* | Forward | GAAGGTCGGAGTCAACGGATTT | 158 |
| | Reverse | GAATTTGCCATGGGTGGAAT | |
| *SLC15A1* | Forward | AGGCTTCACAATAAGCTCAACA | 141 |
| | Reverse | CTTCAAACACCTTCACTTCAGG | |
| *SLC15A2* | Forward | CTTTGGTGCAGCATATCTGTTT | 134 |
| | Reverse | AGCTGTAACCAGGGCATATTGT | |
| *SLC36A1* | Forward | GATCCACCTGTTAAAAGGCAAC | 151 |
| | Reverse | TGAGCACATTTCACCAGGATA | |
| *SLC6A13* | Forward | TTCTACCTCTTCAGCAGCTTCA | 127 |
| | Reverse | GGCATTCTCAGAGGTACCATTC | |

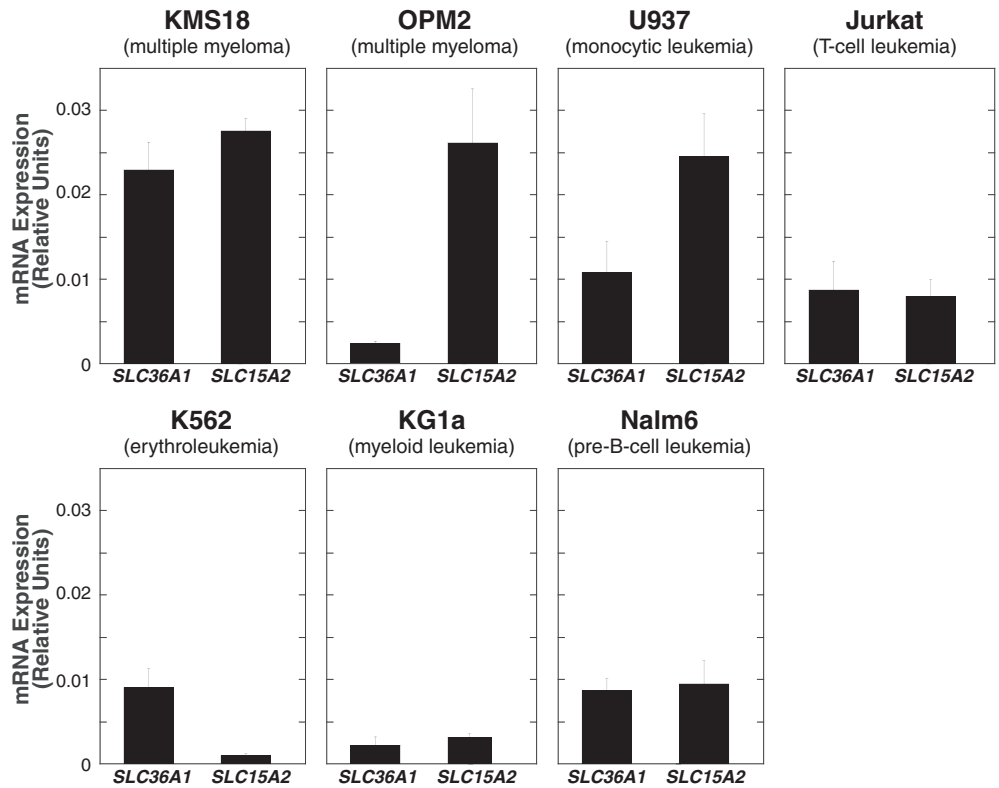


Fig. 1. Expression of ALA transporters in various cell lines of hematological malignancies.
Quantitative RT-PCR analysis of human *SLC36A1*, *SLC15A1*, *SLC15A2*, and *SLC6A13* in KMS18, OPM2, U937, Jurkat, K562, KG1a, and Nalm6 cells. The copy number of each gene relative to that of *GAPDH* was calculated ($n$ = 3, mean ± SE).

transporter (SLC36A1) (Frolund et al. 2010), and a beta transporter (SLC6A13, GABA transporter 2) were used (Bermudez Moretti et al. 2002). Fig. 1 shows that *SLC36A1* and *SLC15A2* were abundantly expressed in KMS18, OPM2, and U937 cells; moderately expressed in Jurkat, K562, and Nalm6 cells; and weakly expressed in KG1a cells. In contrast, expression levels of *SLC15A1* and *SLC6A13* were nearly undetectable in all cell lines (data not shown), which was also similar to that of our previous study based on erythroid cells (Fujiwara et al. 2014).

Next, we evaluated whether PpIX accumulation could be detected using flow cytometry in these cell lines. When 1 mM of ALA was administered for 24 h, KMS18 and OPM2 multiple myeloma cell lines exhibited nearly 100% PpIX positivity (Fig. 2). Moreover, PpIX accumulation was found under the ultraviolet irradiation (Fig. 3A).

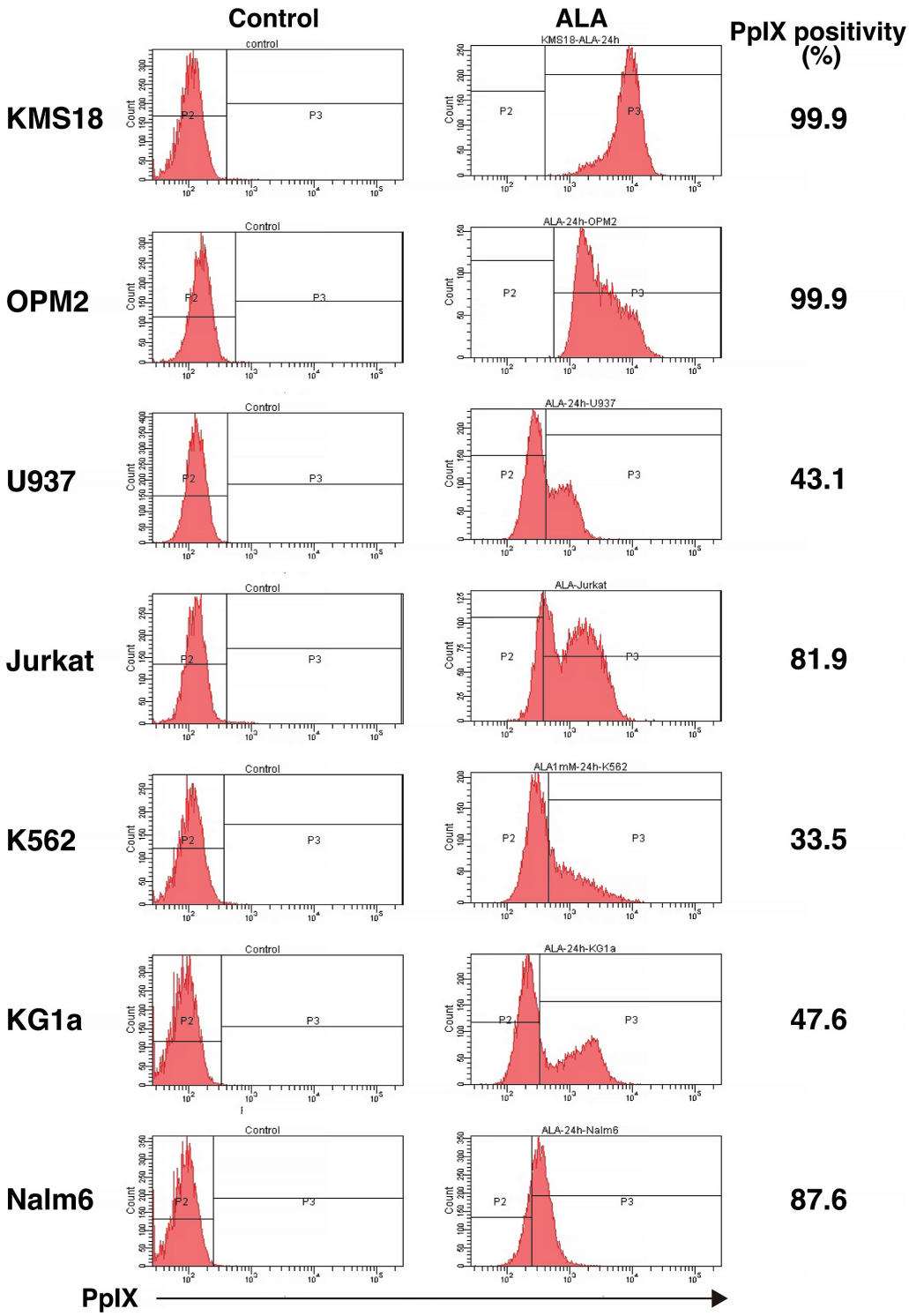


Fig. 2. Flow cytometry-based PpIX detection in ALA-treated various cell lines in hematological malignancies.
Flow cytometric analysis to detect PpIX accumulation in ALA-treated (1 mM, 24 h) cell lines of hematological malignancies. As a control condition, ALA-untreated cells were prepared by parallel culturing. Each plot is representative of two independent experiments, and PpIX positivity is an average of two independent experiments.

However, PpIX positivity in other cell lines varied from 33.5% to 87.6% (Fig. 2). Interestingly, U937, Jurkat, and KG1a cell lines even exhibited the bimodal pattern, and only a subset of K562 and Nalm6 cells showed PpIX positivity (Fig. 2). The cause of various PpIX intensity within a single cell line remains unknown, and a previous study suggested that it was due to the presence of two subpopulations within the Jurkat cell line with distinct miRNA profiles

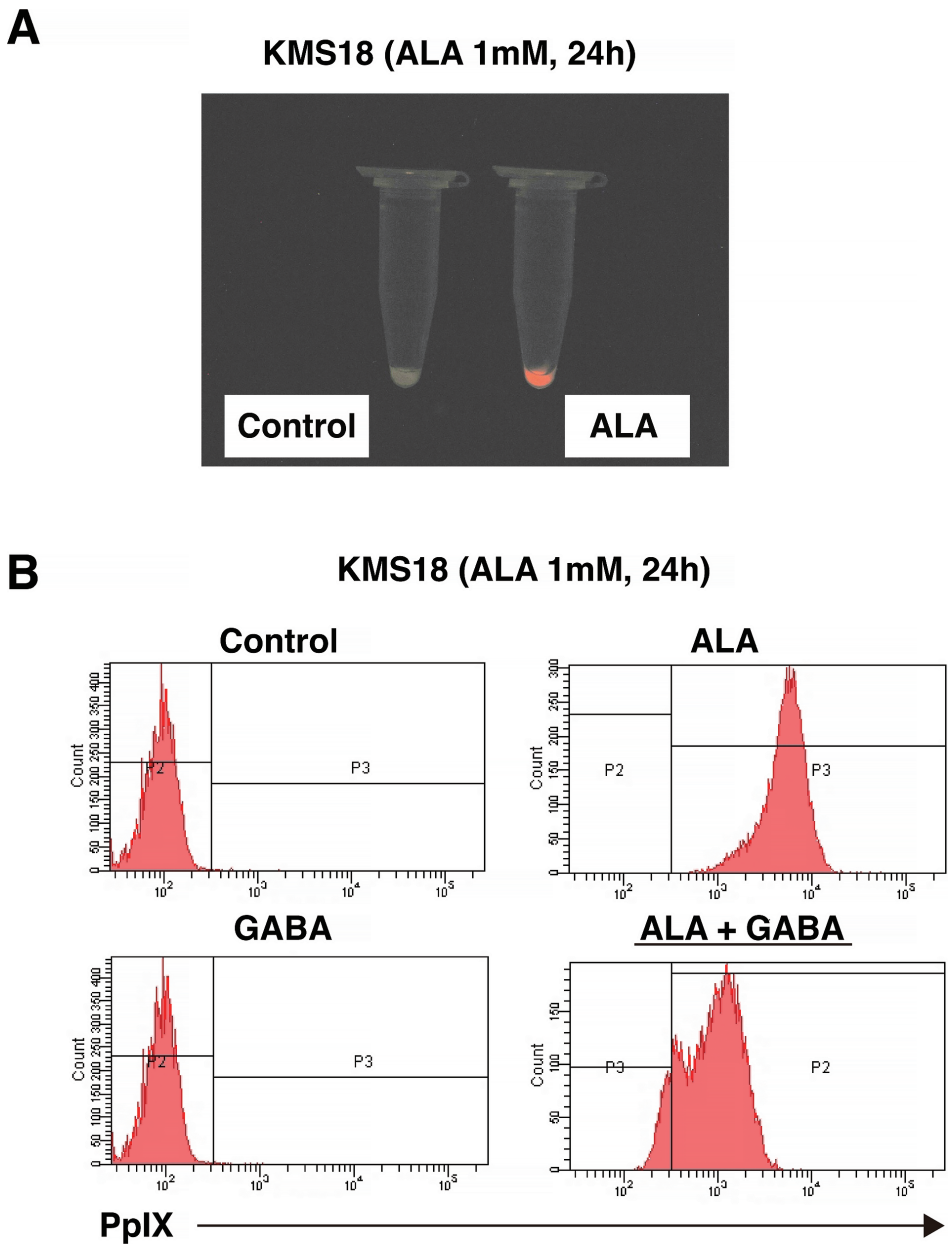


Fig. 3. GABA treatment significantly impedes the effects of ALA in K562 cells.
(A) Ultraviolet irradiated control or ALA-treated KMS18 cells. (B) Flow cytometric analysis to detect PpIX accumulation in the control, ALA, GABA, and ALA+GABA-treated KMS18 cells. ALA and GABA were administered at 1 mM and 40 mM, respectively, for 24 h. Each plot is representative of two independent experiments.

(Erdogan et al. 2018). Another study also demonstrated that it was caused by the karyotypic heterogeneity of the Raji Burkitt lymphoma cell line (Savelyeva and Mamaeva 1988). Thus, the heterogeneity within a subset of each cell line was suspected to contribute to differences in PpIX accumulation capacity.

ALA and GABA are structurally similar; therefore, both of them could serve as SLC36A1 and SLC15A1 substrates (Thwaites et al. 2000; Frolund et al. 2010). Thus, to confirm whether ALA could be incorporated into the KMS18 cells through ALA transporters, GABA was used as a competitive inhibitor of ALA transportation into K562 cells, as previously reported (Frolund et al. 2010). Fig. 3B shows that ALA-mediated PpIX fluorescence was significantly obstructed by GABA treatment.

Although U937 monocytic cells relatively expressed high ALA transporter levels (Fig. 1), ALA-induced PpIX accumulation was less efficient than KMS18 and OPM2 multiple myeloma cell lines (Fig. 2). Therefore, these differences were speculated to be partly due to the differential activities of aerobic glycolysis, known as the "Warburg effect," as previously described (Warburg 1956). Several studies have demonstrated high expression of key regulators of the Warburg effect in myeloma cells, such as lactate

dehydrogenase A (LDHA), pyruvate dehydrogenase kinase 1 (PDK1), and pyruvate kinase M2 (PKM2), to support our hypothesis (Fujiwara et al. 2013; Panchabhai et al. 2017). Alternatively, the possibility that other transporters, or even passive diffusion, might contribute to these differences cannot be completely eliminated. To the best of our knowledges, there is no prior study demonstrating high expression for ALA transporters as well as ALA-induced strong PpIX accumulation in multiple myeloma cells. Thus, further analyses are required to clarify the mechanism behind the accumulation of ALA-induced PpIX in multiple myeloma cell lines.

Therefore, these results suggest that multiple myeloma cells may be a reasonable candidate for ALA-based photodynamic diagnosis.

*Effects of ALA on PpIX accumulation in primary PBMCs*

To determine whether flow cytometry-based photodynamic diagnosis for multiple myeloma could be used as a routine clinical diagnostic method, effects of ALA on PpIX accumulation were tentatively assessed based on primary PBMCs as a normal counterpart. As described, myeloma cell lines have been predicted to more efficiently play a role in the accumulation of PpIX during an ALA treatment than normal PBMCs. When 1 mM of ALA was administered for 24 h, showing nearly 100% PpIX positivity in KMS18 cells (Fig. 2), a significant proportion (12.5%) of primary PBMCs exhibited PpIX positivity (Fig. 4), which makes discrimination between myeloma and normal cells difficult just based on PpIX positivity. Thus, a titration study was conducted based on KMS18 cells to define the optimal ALA concentration and incubation time. As shown in Fig. 5A, PpIX accumulation peaked as early as 2 h of incubation under an ALA concentration of 1 mM. Further, when ALA concentration was titrated by fixing the exposure time of 2 h, nearly all cells (97.7%) exhibited PpIX positivity at the lowest concentration of 0.25 mM, whereas the positivity strongly dropped to 4.4% at the concentration of 0.1 mM (Fig. 5B, C). Moreover, when the incubation time was further shortened to 1 h under the ALA concentration of 0.25 mM, PpIX positivity was strongly decreased (9.5%; Fig. 5C).

When primary PBMC was treated with ALA at 0.25 mM for 2 h, only 1.8% of the cells were found to weakly show PpIX positivity (Figs. 5C, 6A). However, with further reduction of ALA exposure (0.25 mM for 1 h, 0.1 mM for 1 or 2 h) could obviously suppress PpIX positivity in PBMCs (0.2-0.9%), the PpIX positivity in KMS18 was also strongly suppressed (Fig. 5C). Higher ALA concentration and shorter exposure time, such as 1 mM for 1 h, might possibly discriminate myeloma and normal cells. However, previous studies indicated that ALA treatment at higher concentration (0.5-1 mM) significantly compromised the proliferation of K562 cells (Pluskalova et al. 2006; Fujiwara et al. 2014), implying that higher ALA concentration might be toxic on both myeloma cells and perhaps on primary PBMCs and thus could negatively affect the accuracy of MRD detection. Thus, we favored that ALA treatment of 0.25 mM for 2h would be an optimal dose to discriminate myeloma and normal cells. Based on the preferential PpIX accumulation in myeloma cells (Figs. 1, 5, 6), we suppose that our method would be able to detect very low number of myeloma cells in the bone marrow. However, it should be important to estimate the sensitivity of ALA-based MRD detection technique by evaluating the ALA-induced PpIX positivity based on a mixture of myeloma cells and PBMCs at a different ratio (i.e., myeloma/PBMCs = 1/100, 1/1,000 or 1/10,000), and compare with the existing techniques, including multicolor flow cytometry- and next-generation sequencing-based MRD detections.

Finally, the cellular component among PBMCs showing PpIX positivity was defined. As shown in Fig. 6B, a cell fraction showing higher forward scatter (FSC)/side scatter (SSC) (P2) exhibited PpIX positivity, whereas the cell fraction showing lower FSC/SSC (P1) did not accumulate PpIX upon ALA treatment. As lower FSC/SSC expresses CD3 or CD19, the fraction would correspond to peripheral lymphocytes (Fig. 6C). On the contrary, a subset

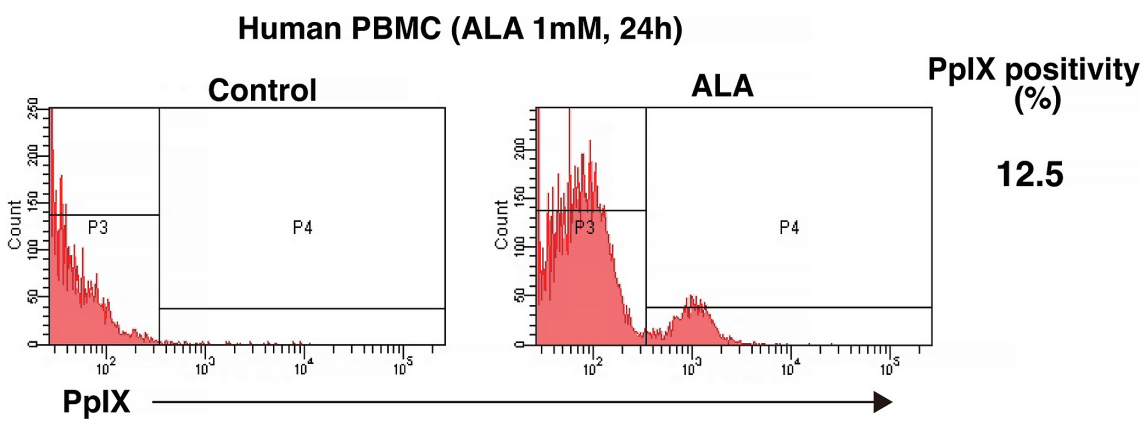


Fig. 4. Significant PpIX accumulation in primary PBMCs after ALA exposure.
Flow cytometric analysis to detect PpIX accumulation in ALA-treated (1 mM, 24 h) PBMCs. As a control condition, ALA-untreated cells were prepared by parallel culturing. Each plot is representative of two independent experiments.

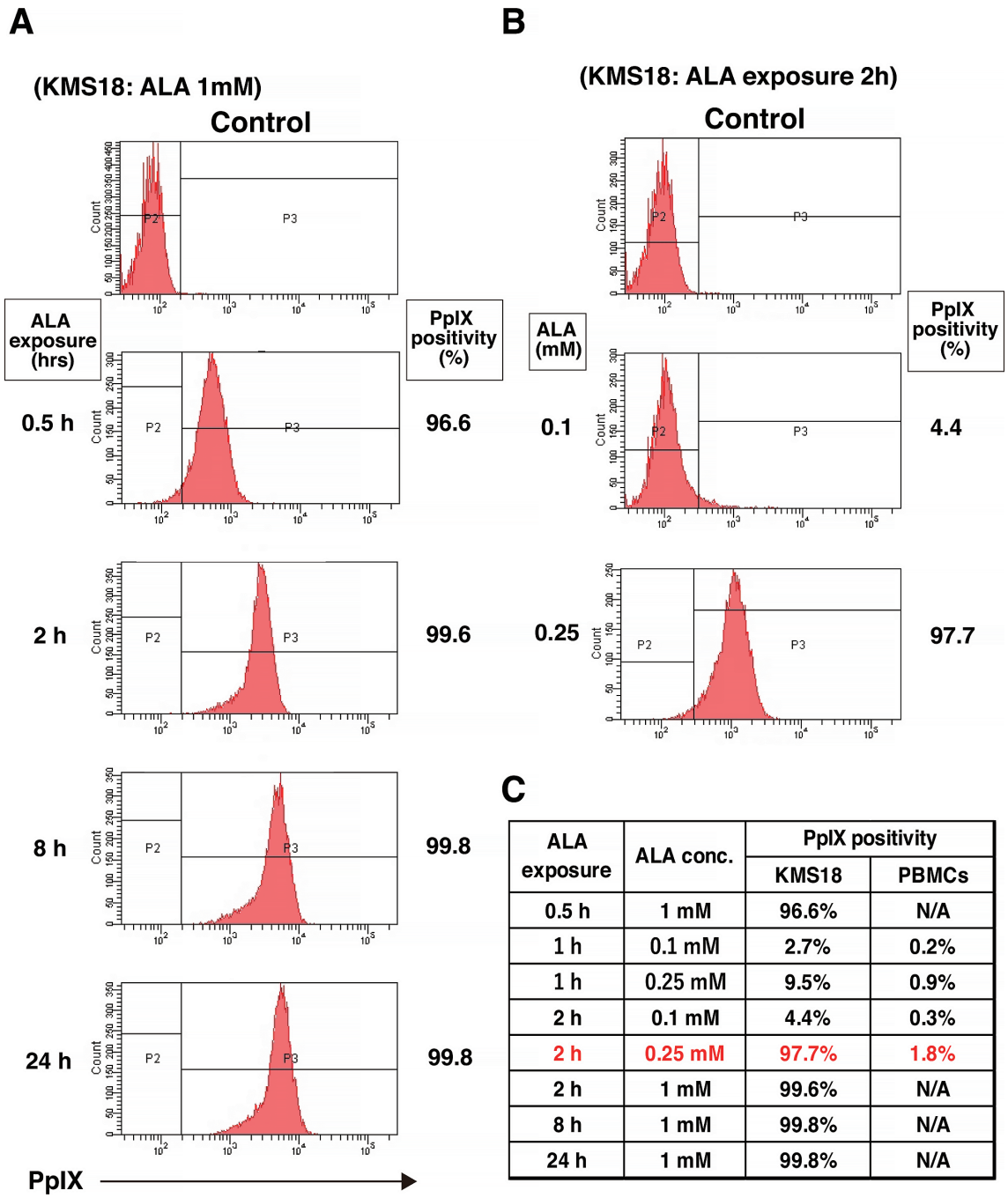


C

| ALA exposure | ALA conc. | PpIX positivity | |
|---|---|---|---|
| | | KMS18 | PBMCs |
| 0.5 h | 1 mM | 96.6% | N/A |
| 1 h | 0.1 mM | 2.7% | 0.2% |
| 1 h | 0.25 mM | 9.5% | 0.9% |
| 2 h | 0.1 mM | 4.4% | 0.3% |
| 2 h | 0.25 mM | 97.7% | 1.8% |
| 2 h | 1 mM | 99.6% | N/A |
| 8 h | 1 mM | 99.8% | N/A |
| 24 h | 1 mM | 99.8% | N/A |

Fig. 5. Titration study of ALA treatment in KMS18 cells and PBMCs.
(A) ALA exposure time was titrated under the ALA concentration of 1 mM. Each plot is representative of two independent experiments. (B) ALA concentration was titrated under ALA exposure time of 2 h. Each plot is representative of two independent experiments. (C) Summary of ALA titration study. PpIX positivity is an average of two independent experiments.

of higher FSC/SSC fraction was found to express CD14 (Fig. 6C), indicating that a monocyte fraction may tend to accumulate PpIX after an ALA exposure. However, to the best of our knowledge, neither the ALA effect on PpIX accumulation nor expressions for ALA transporter in normal monocytes have been demonstrated, which would warrant further investigation. In contrast, some studies suggested that both SLC15A1 and SLC15A2 were expressed in macrophages (Ayyadurai et al. 2013; Hu et al. 2018), which could be partly derived from bone marrow monocytes (Varol et al. 2015). Interestingly, heme could promote monocyte differentiation into macrophages by inducing the transcription factor SPI-C (Haldar et al. 2014). Thus, we could not ignore the possibility that ALA-mediated enhanced the heme synthesis in monocytes that might upregulate ALA transporters by specifying macrophage dif-

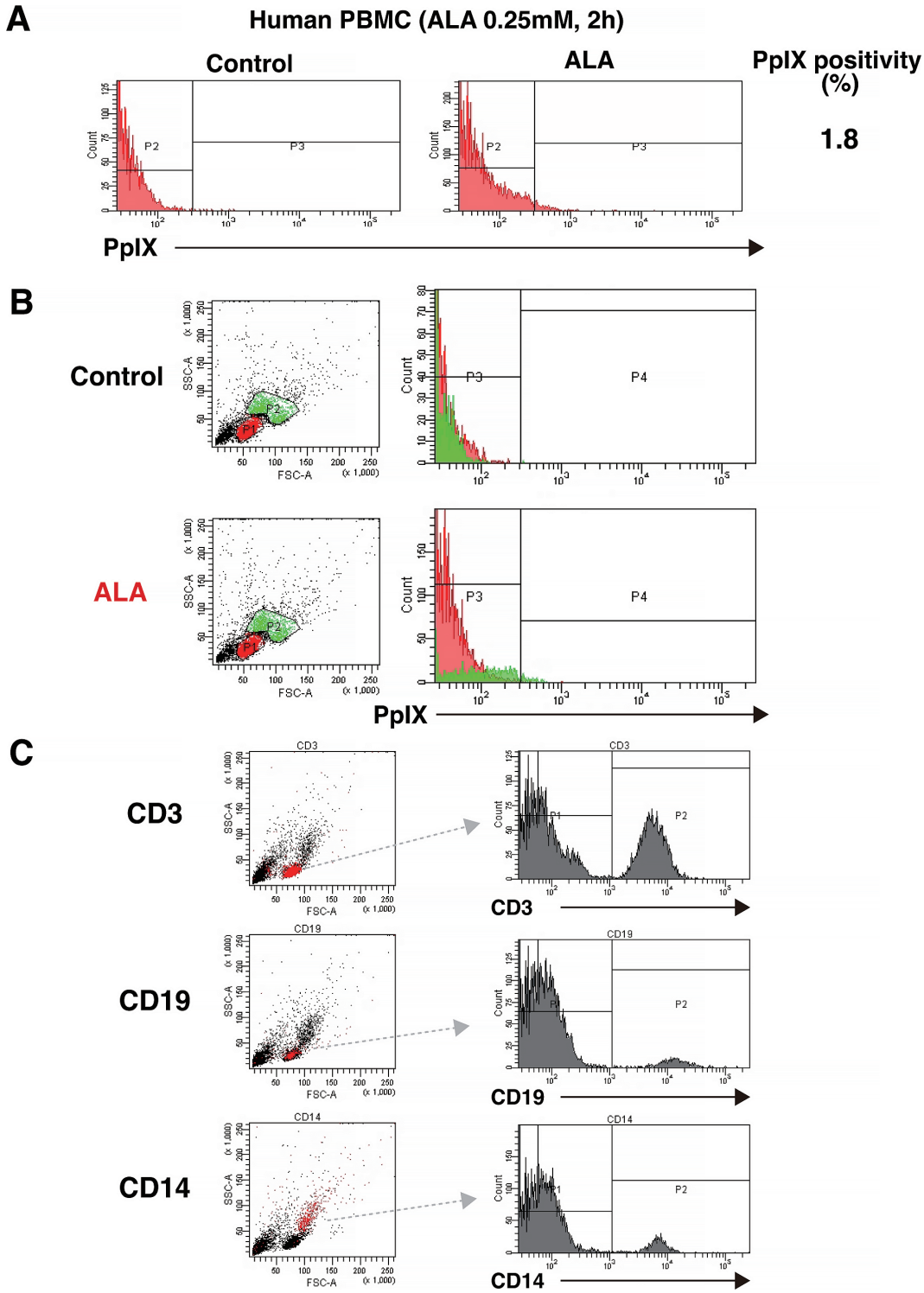


Fig. 6. Evaluation of PpIX-positive PBMC fraction.
(A) Flow cytometric analysis to detect PpIX accumulation in ALA-treated (0.25 mM, 2 h) PBMCs. Each plot is representative of two independent experiments. (B) Identification of PpIX-positive cell fraction among PBMCs. A cell fraction showing higher FSC forward scatter (FSC)/side scatter (SSC) (P2) exhibited PpIX positivity and expressed CD14, whereas the cell fraction showing lower FSC/SSC (P1) did not accumulate PpIX upon ALA treatment. (C) The cell fraction showing lower FSC/SSC (P1) expressed CD3 or CD19, while the cell fraction showing higher FSC/SSC (P2) expressed CD14.

ferentiation, thereby contributing to detectable PpIX fluorescence within a subset of higher FSC/SSC fraction.

A limitation of this study is that only a small subset (1.8%) of normal PBMCs exhibited PpIX positivity even in the titration study (Figs. 5, 6). In this regard, a previous fundamental investigation for the detection of circulating tumor cells, such as colon and gastric cancers, combining the epithelial cell marker EpCAM (Epithelial cell adhesion molecule, CD326) was applied in the ALA-based photodynamic diagnosis, which might efficiently discriminate peripheral blood and cancer cells (Matsusaka et al. 2014). However, myeloma cells did not express EpCAM, and thus, future identification of specific markers might be preferred. Another limitation is that we only aimed to discriminate myeloma cell lines and primary PBMCs: the use of bone marrow samples derived from patients with multiple myeloma would be important, because residual myeloma cells might be preferentially observed in the bone marrow niche. Whereas the combination of plasma cell markers (CD138 and CD38) and additional markers (i.e., CD19, CD27, CD45, CD56, CD81, and CD117) is used to discriminate normal and clonal plasma cells, normal plasma cells could exhibit a considerably heterogenous immunophenotype according to their maturation process (Mei et al. 2009; Paiva et al. 2015). Also, CD38 negative multiple myeloma could be observed following the treatment including daratumumab (human monoclonal anti-CD38 directed antibody) (Mykytiv et al. 2019). Therefore, further investigations of the feasibility of ALA-based photodynamic diagnosis based on the bone marrow samples are required to overcome these potential limitations.

In conclusion, these results indicate the potential usefulness of flow cytometry-based photodynamic diagnosis for the detection of MRD in multiple myeloma.

## Acknowledgments

We are grateful to Drs. Masahiro Ishizuka and Kiwamu Takahashi (SBI Pharmaceuticals Co., Ltd.) for their helpful comments. This manuscript is supported by JSPS KAKENHI Grant No. 16K15324 (H.H.).

## Conflict of Interest

The authors declare no conflict of interest.

## References

Ahlin, G., Hilgendorf, C., Karlsson, J., Szigyarto, C.A., Uhlen, M. & Artursson, P. (2009) Endogenous gene and protein expression of drug-transporting proteins in cell lines routinely used in drug discovery programs. *Drug Metab. Dispos.*, **37**, 2275-2283.

Anderson, K.C., Auclair, D., Kelloff, G.J., Sigman, C.C., Avet-Loiseau, H., Farrell, A.T., Gormley, N.J., Kumar, S.K., Landgren, O., Munshi, N.C., Cavo, M., Davies, F.E., Di Bacco, A., Dickey, J.S., Gutman, S.I., et al. (2017) The role of minimal residual disease testing in myeloma treatment selection and drug development: current value and future applications. *Clin. Cancer Res.*, **23**, 3980-3993.

Ayyadurai, S., Charania, M.A., Xiao, B., Viennois, E. & Merlin, D. (2013) PepT1 expressed in immune cells has an important role in promoting the immune response during experimentally induced colitis. *Lab. Invest.*, **93**, 888-899.

Bermudez Moretti, M., Correa Garcia, S., Perotti, C., Batlle, A. & Casas, A. (2002) Delta-aminolevulinic acid transport in murine mammary adenocarcinoma cells is mediated by beta transporters. *Br. J. Cancer*, **87**, 471-474.

Erdogan, I., Cosacak, M.I., Nalbant, A. & Akgul, B. (2018) Deep sequencing reveals two Jurkat subpopulations with distinct miRNA profiles during camptothecin-induced apoptosis. *Turk. J. Biol.*, **42**, 113-122.

Frolund, S., Marquez, O.C., Larsen, M., Brodin, B. & Nielsen, C.U. (2010) Delta-aminolevulinic acid is a substrate for the amino acid transporter SLC36A1 (hPAT1). *Br. J. Pharmacol.*, **159**, 1339-1353.

Fujiwara, S., Kawano, Y., Yuki, H., Okuno, Y., Nosaka, K., Mitsuya, H. & Hata, H. (2013) PDK1 inhibition is a novel therapeutic target in multiple myeloma. *Br. J. Cancer*, **108**, 170-178.

Fujiwara, T., Okamoto, K., Niikuni, R., Takahashi, K., Okitsu, Y., Fukuhara, N., Onishi, Y., Ishizawa, K., Ichinohasama, R., Nakamura, Y., Nakajima, M., Tanaka, T. & Harigae, H. (2014) Effect of 5-aminolevulinic acid on erythropoiesis: a preclinical in vitro characterization for the treatment of congenital sideroblastic anemia. *Biochem. Biophys. Res. Commun.*, **454**, 102-108.

Furuyama, K., Kaneko, K. & Vargas, P.D. (2007) Heme as a magnificent molecule with multiple missions: heme determines its own fate and governs cellular homeostasis. *Tohoku J. Exp. Med.*, **213**, 1-16.

Gambella, M., Omede, P., Spada, S., Muccio, V.E., Gilestro, M., Saraci, E., Grammatico, S., Larocca, A., Conticello, C., Bernardini, A., Gamberi, B., Troia, R., Liberati, A.M., Offidani, M., Rocci, A., et al. (2019) Minimal residual disease by flow cytometry and allelic-specific oligonucleotide real-time quantitative polymerase chain reaction in patients with myeloma receiving lenalidomide maintenance: a pooled analysis. *Cancer*, **125**, 750-760.

Gibbs, S.L., Chen, B., O'Hara, J.A., Hoopes, P.J., Hasan, T. & Pogue, B.W. (2006) Protoporphyrin IX level correlates with number of mitochondria, but increase in production correlates with tumor cell size. *Photochem. Photobiol.*, **82**, 1334-1341.

Haldar, M., Kohyama, M., So, A.Y., Kc, W., Wu, X., Briseno, C.G., Satpathy, A.T., Kretzer, N.M., Arase, H., Rajasekaran, N.S., Wang, L., Egawa, T., Igarashi, K., Baltimore, D., Murphy, T.L., et al. (2014) Heme-mediated SPI-C induction promotes monocyte differentiation into iron-recycling macrophages. *Cell*, **156**, 1223-1234.

Hu, Y., Song, F., Jiang, H., Nunez, G. & Smith, D.E. (2018) SLC15A2 and SLC15A4 mediate the transport of bacterially derived di/tripeptides to enhance the nucleotide-binding oligomerization domain-dependent immune response in mouse bone marrow-derived macrophages. *J. Immunol.*, **201**, 652-662.

Ingersoll, S.A., Ayyadurai, S., Charania, M.A., Laroui, H., Yan, Y. & Merlin, D. (2012) The role and pathophysiological relevance of membrane transporter PepT1 in intestinal inflammation and inflammatory bowel disease. *Am. J. Physiol. Gastrointest. Liver Physiol.*, **302**, G484-492.

Ishizuka, M., Abe, F., Sano, Y., Takahashi, K., Inoue, K., Nakajima, M., Kohda, T., Komatsu, N., Ogura, S. & Tanaka, T. (2011) Novel development of 5-aminolevurinic acid (ALA) in cancer diagnoses and therapy. *Int. Immunopharmacol.*, **11**, 358-365.

Matsusaka, S., Kozuka, M., Takagi, H., Ito, H., Minowa, S., Hirai, M. & Hatake, K. (2014) A novel detection strategy for living circulating tumor cells using 5-aminolevulinic acid. *Cancer Lett.*, **355**, 113-120.

Mei, H.E., Yoshida, T., Sime, W., Hiepe, F., Thiele, K., Manz, R.A., Radbruch, A. & Dorner, T. (2009) Blood-borne human plasma

cells in steady state are derived from mucosal immune responses. *Blood*, **113**, 2461-2469.
Mykytiv, V., Alwaheed, A. & Mohd Hashim, N.A. (2019) Double CD38(−)/CD138(−) negative multiple myeloma. *Hematol. Oncol. Stem Cell Ther.*, **12**, 64-66.
Nokes, B., Apel, M., Jones, C., Brown, G. & Lang, J.E. (2013) Aminolevulinic acid (ALA): photodynamic detection and potential therapeutic applications. *J. Surg. Res.*, **181**, 262-271.
Paiva, B., van Dongen, J.J. & Orfao, A. (2015) New criteria for response assessment: role of minimal residual disease in multiple myeloma. *Blood*, **125**, 3059-3068.
Panchabhai, S., Schlam, I., Sebastian, S. & Fonseca, R. (2017) PKM2 and other key regulators of Warburg effect positively correlate with CD147 (EMMPRIN) gene expression and predict survival in multiple myeloma. *Leukemia*, **31**, 991-994.
Pluskalova, M., Peslova, G., Grebenova, D., Halada, P. & Hrkal, Z. (2006) Photodynamic treatment (ALA-PDT) suppresses the expression of the oncogenic Bcr-Abl kinase and affects the cytoskeleton organization in K562 cells. *J. Photochem. Photobiol. B*, **83**, 205-212.
Saito, Y., Fujiwara, T., Ohashi, K., Okitsu, Y., Fukuhara, N., Onishi, Y., Ishizawa, K. & Harigae, H. (2015) High-throughput siRNA screening to reveal GATA-2 upstream transcriptional mechanisms in hematopoietic cells. *PLoS One*, **10**, e0137079.
Savelyeva, L. & Mamaeva, S. (1988) Population analysis of karyotypic heterogeneity of the Raji Burkitt lymphoma cell line. Analysis of 100 karyotypes. *Cancer Genet. Cytogenet.*, **34**, 63-75.
Thwaites, D.T., Basterfield, L., McCleave, P.M., Carter, S.M. & Simmons, N.L. (2000) Gamma-aminobutyric acid (GABA) transport across human intestinal epithelial (Caco-2) cell monolayers. *Br. J. Pharmacol.*, **129**, 457-464.
Varol, C., Mildner, A. & Jung, S. (2015) Macrophages: development and tissue specialization. *Annu. Rev. Immunol.*, **33**, 643-675.
Warburg, O. (1956) On the origin of cancer cells. *Science*, **123**, 309-314.